

SEVENTY-ONE NEW L AND T DWARFS FROM THE SLOAN DIGITAL SKY SURVEY

K. CHIU¹, X. FAN², S. K. LEGGETT³, D. A. GOLIMOWSKI¹,
W. ZHENG¹, T. R. GEBALLE⁴, D. P. SCHNEIDER⁵, J. BRINKMANN⁶*Accepted by AJ*

ABSTRACT

We present near-infrared observations of 71 newly discovered L and T dwarfs, selected from imaging data of the Sloan Digital Sky Survey (SDSS) using the *i*-dropout technique. Sixty-five of these dwarfs have been classified spectroscopically according to the near-infrared L dwarf classification scheme of Geballe et al. and the unified T dwarf classification scheme of Burgasser et al. The spectral types of these dwarfs range from L3 to T7, and include the latest types yet found in the SDSS. Six of the newly identified dwarfs are classified as early- to mid-L dwarfs according to their photometric near-infrared colors, and two others are classified photometrically as M dwarfs. We also present new near-infrared spectra for five previously published SDSS L and T dwarfs, and one L dwarf and one T dwarf discovered by Burgasser et al. from the Two Micron All Sky Survey. The new SDSS sample includes 27 T dwarfs and 30 dwarfs with spectral types spanning the complex L–T transition (L7–T3). We continue to see a large (~ 0.5 mag) spread in J – H for L3 to T1 types, and a similar spread in H – K for all dwarfs later than L3. This color dispersion is probably due to a range of grain sedimentation properties, metallicity, and gravity. We also find L and T dwarfs with unusual colors and spectral properties that may eventually help to disentangle these effects.

Subject headings: infrared: stars — stars: low-mass, brown dwarfs

1. INTRODUCTION

Over the last decade, the search for rare astronomical objects has undergone an explosion of productivity, thanks in part to the specialized labor associated with modern digital sky surveys. Innovative programmers and instrumentalists designing highly automated software pipelines and large imaging arrays have laid the groundwork for massive databases that can now be mined for objects once only thought to exist. The result of these efforts has been the most productive period in history for the discovery of rare objects, which range from the brightest and most distant quasars (Fan et al. 1999, 2000a, 2001a,b, 2003, 2004; Zheng et al. 2000) to the faintest and nearest stars and brown dwarfs (Kirkpatrick et al. 1999; Burgasser et al. 1999; Kirkpatrick et al. 2000; Fan et al. 2000b; Leggett et al. 2000; Burgasser et al. 2002a; Geballe et al. 2002, hereafter G02; Knapp et al. 2004, hereafter K04).

Since the first discoveries of L and T dwarfs in the early 1990s, the ranks of these spectral classes have been populated through systematic searches of large-area, optical and near-infrared surveys such as the Deep Near Infrared Survey of the Southern Sky (DENIS; Epchtein 1997), the Two Micron All Sky Survey (2MASS; Skrutskie et al. 1997), and the Sloan Digital Sky Survey (SDSS; York et al. 2000). Although time intensive, these searches are more productive and efficient than the tedious, pointed surveys that pre-

ceded them. The optical and near-infrared spectra of the many known L and T dwarfs have yielded well-defined classification schemes and valuable information about the chemical compositions, temperatures, and other physical characteristics of ultracool dwarfs (Kirkpatrick et al. 2000; Burgasser et al. 2002a, 2005; G02; K04; Golimowski et al. 2004a).

L and T dwarfs, which link the lowest mass stars and the highest mass planets, are the subjects of a broad range of observational and theoretical studies (Kirkpatrick 2005). A principal goal of these studies is the determination of the substellar mass function, which is fundamental to understanding the star formation process at the lowest mass end and how it is related to the formation and evolution of planetary systems (Burgasser et al. 2004b; Allen et al. 2005). The hundreds of L dwarfs and more than 50 T dwarfs discovered from 2MASS and SDSS data compose a statistical sample of brown dwarfs essential to understanding the demographics and eventually the luminosity and mass functions of substellar objects (Fan et al., in prep.).

Since 1999, we have used SDSS imaging data to select L and T dwarf candidates and carry out follow-up observations of their photometric and spectroscopic properties (Strauss et al. 1999; Tsvetanov et al. 2000; Fan et al. 2000b; Leggett et al. 2000, 2002; Schneider et al. 2002; G02; Hawley et al. 2002; K04; Golimowski et al. 2004a). The SDSS i – z color, which is our primary selection criterion, is sensitive to brown dwarfs of all effective temperatures as long as they are bright enough to be detected in the z band. Near-infrared selection criteria, such as those employed by the 2MASS group (e.g., Burgasser et al. 2002a), are more sensitive to late-T dwarfs which are optically faint, but they are less efficient in detecting dwarfs at the L–T transition because their near-infrared colors are indistinguishable from those of the more numerous M dwarfs. Therefore, the SDSS selection criterion is better

¹ Department of Physics and Astronomy, The Johns Hopkins University, 3400 North Charles Street, Baltimore, MD 21218, USA

² Steward Observatory, The University of Arizona, Tucson, AZ 85721

³ United Kingdom Infrared Telescope, Joint Astronomy Center, 660 North A'ohoku Place, Hilo, Hawaii 96720

⁴ Gemini Observatory, 670 North A'ohoku Place, Hilo, HI 96720

⁵ Department of Astronomy and Astrophysics, Pennsylvania State University, 525 Davey Laboratory, University Park, PA 16802

⁶ Apache Point Observatory, P.O. Box 59, Sunspot, NM 88349

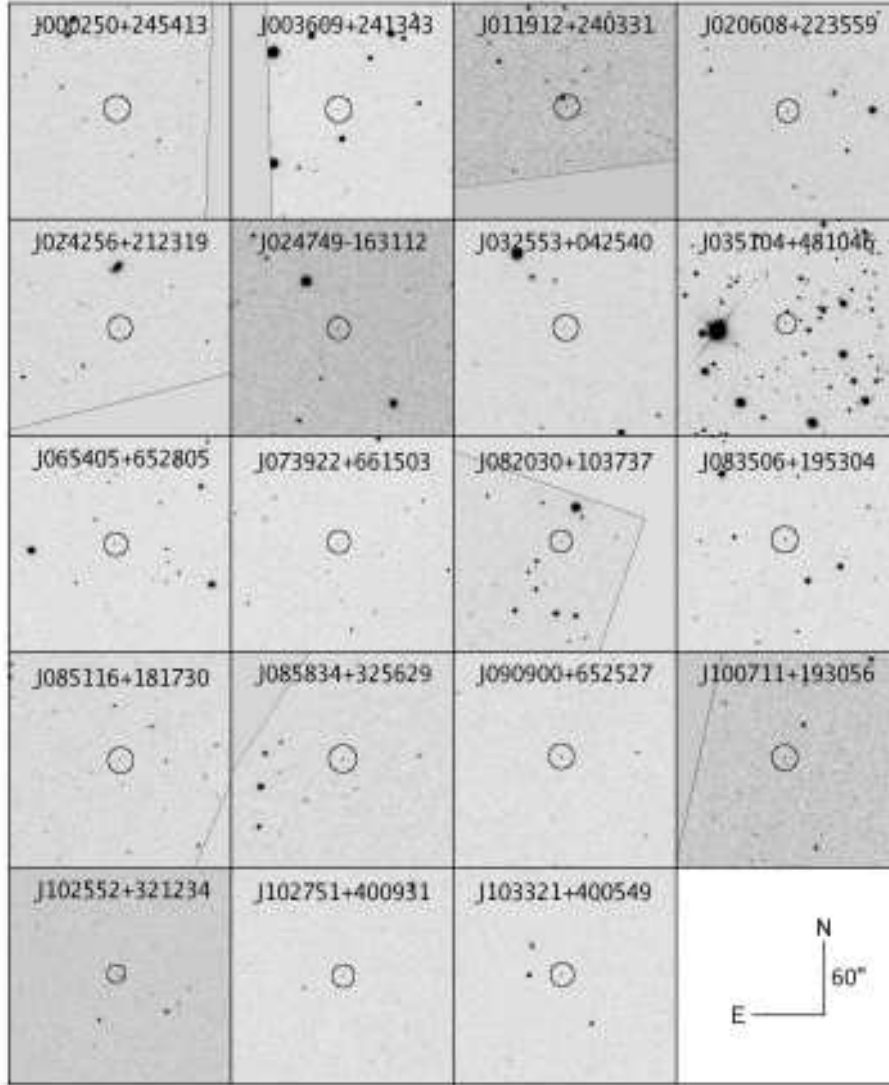


FIG. 1.— SDSS z finding charts for the 73 new M, L, and T dwarfs found in this work. North is up, East is left. The fields of view are $3' \times 3'$. (Full resolution versions of these finding charts will appear in the published journal edition.)

suited for defining a complete, magnitude-limited sample of field brown dwarfs.

In this paper, we report the discovery and properties of 71 L and T dwarfs drawn from over 3500 deg^2 of SDSS imaging data. We describe the techniques for identifying and confirming these dwarfs based on their SDSS and near-infrared colors. We classify 65 of the L and T dwarfs from their near-infrared spectra, and we identify 6 L dwarfs and 2 M dwarfs from their photometric colors. The observations are presented in §2, spectral classification of the sample is presented in §3, and variations in the photometric and spectroscopic properties are discussed in §4. Our conclusions are given in §5.

2. OBSERVATIONS

The search for nearby, ultracool dwarfs at optical wavelengths is fortuitously related to the search for the most distant galaxies and quasars in the universe. Because both types of objects have very red optical colors caused by rising flux into the near-infrared, a search for one yields the other (or from another perspective, one is the

unwanted contaminant of the other). The “ i -dropout” and related techniques have been employed in nearly all high-redshift observing programs, so a joint effort to find L and T dwarfs with these techniques benefits both programs.

2.1. General Selection Method

We select candidate L and T dwarfs using the i and z magnitudes of sources listed in the SDSS photometric catalog. The SDSS uses a dedicated 2.5 m telescope in a drift-scanning mode to acquire digital images. The hardware and software pipelines that produce the final astrometry and photometry have been described by the project collaborators elsewhere in detail: Fukugita et al. (1996), Gunn et al. (1998), Hogg et al. (2001), Lupton et al. (1999), Stoughton et al. (2002), Smith et al. (2002), Pier et al. (2003), and Abazajian et al. (2004).

Fan et al. (2001b) described the i -dropout selection and identification procedures used in this program. The

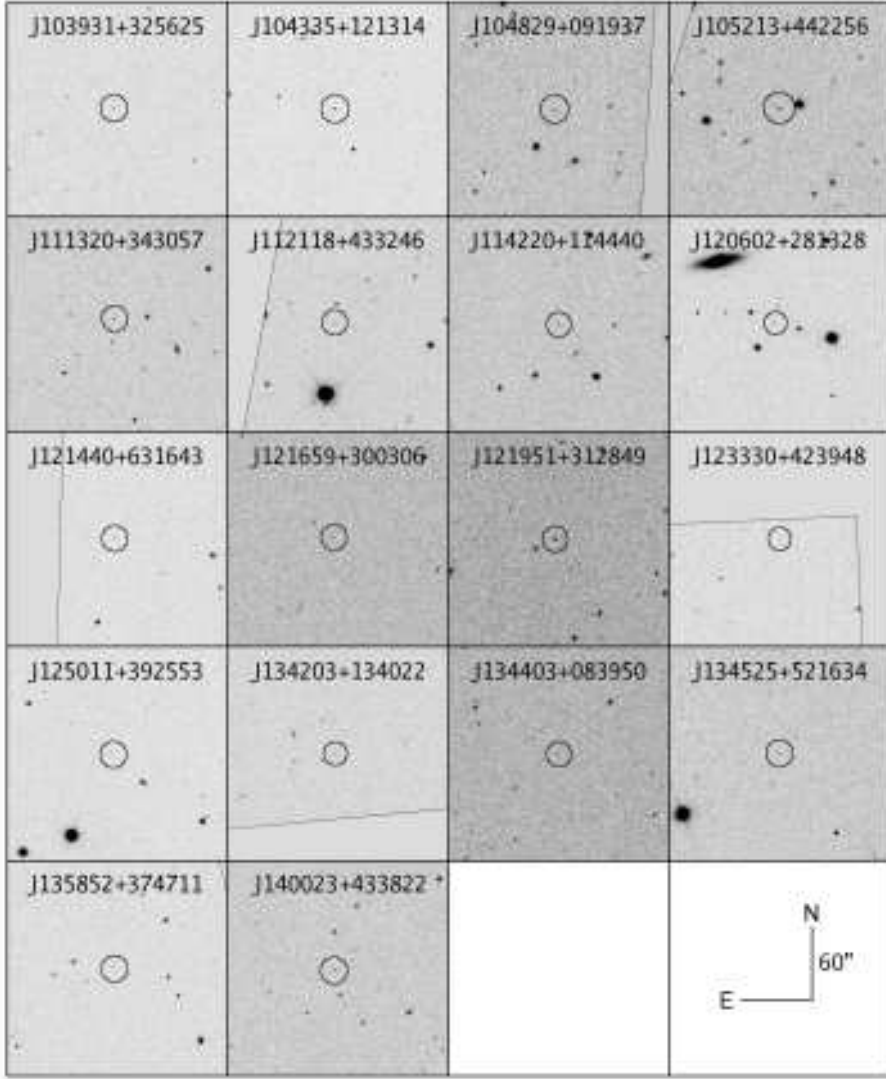


FIG. 1.— (continued) SDSS z finding charts for the 73 new M, L, and T dwarfs found in this work. North is up, East is left. The fields of view are $3' \times 3'$. (Full resolution versions of these finding charts will appear in the published journal edition.)

photometric selection criteria are:

$$\begin{aligned} z &< 20.4, \\ \sigma(z) &< 0.12, \\ i - z &> 2.2. \end{aligned} \quad (1)$$

Because most of the SDSS area is imaged only once and our i -dropout technique favors one-band detections, our initial list of L and T dwarf candidates is heavily contaminated by cosmic rays. False detections from cosmic rays and intrinsic faintness are the main problems preventing the SDSS itself from discovering these objects, as well as $z > 5.7$ quasars, in its automated spectroscopic observing program (Richards et al. 2002). We conservatively remove cosmic rays from our list by visual inspection.

The reality of the remaining bright candidates can be immediately confirmed by correlating the list with the 2MASS All-Sky Point Source Catalog, which contains near-infrared photometry down to a 10σ detection limit of $J = 15.8$. We matched our SDSS candidates with 2MASS sources, allowing for small astrometric errors

caused by the proper motions of these nearby dwarfs. Although the $z-J$ colors of ultracool dwarfs are very red ($z-J > 2$; Fan et al. 2001b), our fainter candidates often do not appear in the 2MASS catalog because of 2MASS's shallower imaging depth. Those fainter candidates not confirmed by 2MASS were further examined through independent J -band imaging. Additional SDSS i and z imaging was carried out to secure our primary color criterion of $i-z > 2.2$.

The followup J -band photometry allows us to distinguish very red L and T dwarf candidates from bluer high-redshift quasar candidates. Quasars at redshifts > 5.7 have $z-J < 1.5$ because their intrinsic continua are dominated by a blue power law. Ultracool dwarfs are more easily discovered than quasars because they are much redder, and therefore, significantly brighter in the J band. Applying the selection criteria above to a 6600 deg^2 survey area, we have confirmed 53 T dwarfs and over 100 L dwarfs (including those found in this work), but only 19 quasars with redshifts > 5.7 .

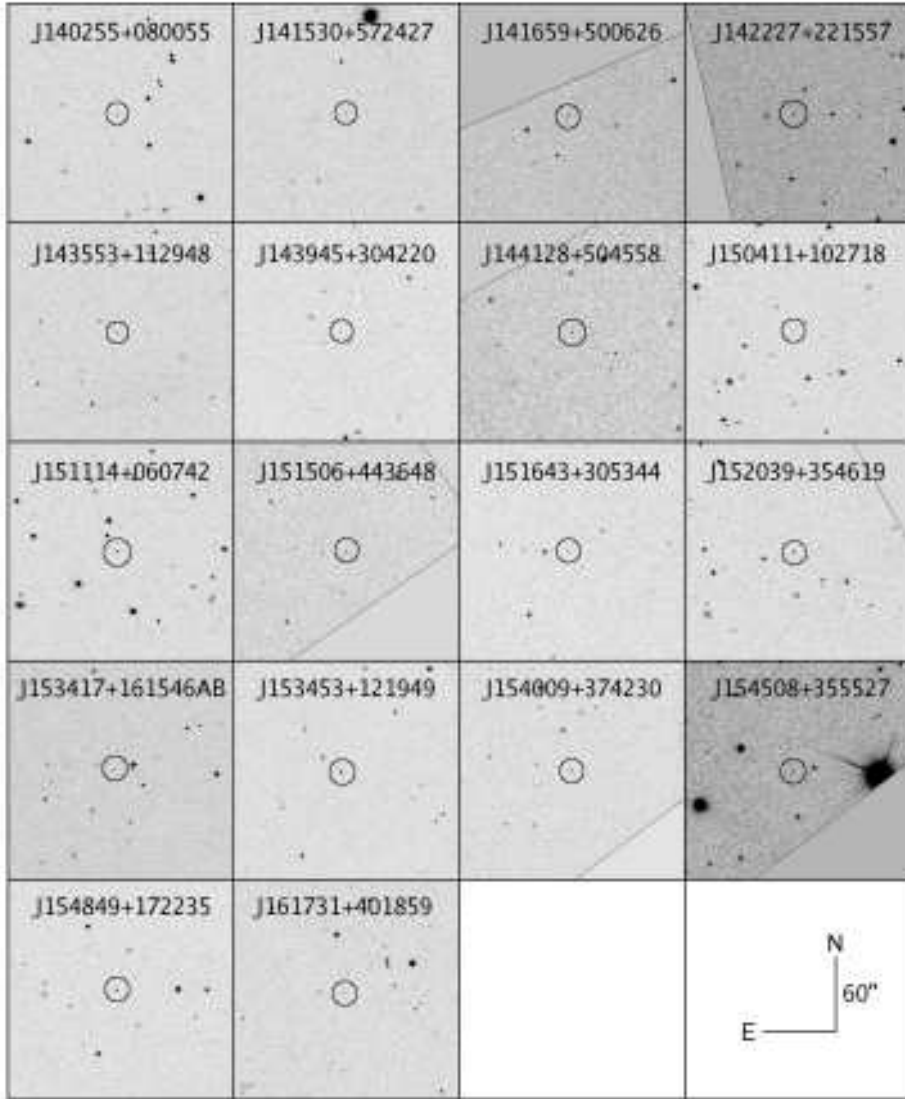


FIG. 1.— (continued) SDSS z finding charts for the 73 new M, L, and T dwarfs found in this work. North is up, East is left. The fields of view are $3' \times 3'$. (Full resolution versions of these finding charts will appear in the published journal edition.)

Finally, we obtained near-infrared spectra of candidates whose colors matched those of L and T dwarfs, at the wavelength resolution needed to determine the dwarf classification indices.

2.2. Photometric Observations

The area of sky covered in this work is 3526 deg^2 , comprising imaging runs recorded from early 2003 to 2005 and a few earlier runs that had been reprocessed through the SDSS photometric pipeline. Eighty four i -dropout candidates were selected using the criteria in Equation (1), and then examined with the 2MASS catalog or follow-up z and J imaging. A few additional candidates with attributes outside of our formal selection limits were also selected, in order to fill gaps during observations. We obtained z -band images with the SPI-CAM imager on the Astrophysical Research Consortium (ARC) 3.5 m telescope at the Apache Point Observatory. The typical exposure time needed to verify the presence of a $z = 20.4$ source was ~ 60 s. We obtained J -band

images with the 256×256 NICMOS camera on Steward Observatory's 2.3 m Bok Telescope, and the GRIM II and NIC-FPS imagers on the ARC 3.5 m telescope.

Candidates surviving our initial photometric screening were then imaged through the Mauna Kea Observatory (MKO) J , H , and K bands (Simons & Tokunaga 2002; Tokunaga et al. 2002) using the United Kingdom Infrared Telescope (UKIRT) Fast-Track Imager (UFTI; Roche et al. 2003) or the NASA Infrared Telescope Facility (IRTF) imager/spectrometer SpeX (Rayner et al. 2003). UKIRT Faint Standards (Hawarden et al. 2001) were used to calibrate the data. Typical exposure times were 60 s, with a five or nine point dither pattern.

Table 1 lists the SDSS designations, SDSS iz and MKO JHK magnitudes, and observation details for the 73 M, L, and T dwarfs discovered in this work.⁷ Although the

⁷ The SDSS iz magnitudes are based on the AB system, whereas the MKO JHK magnitudes are based on the Vega system. The photometric errors of these objects in the SDSS public data releases

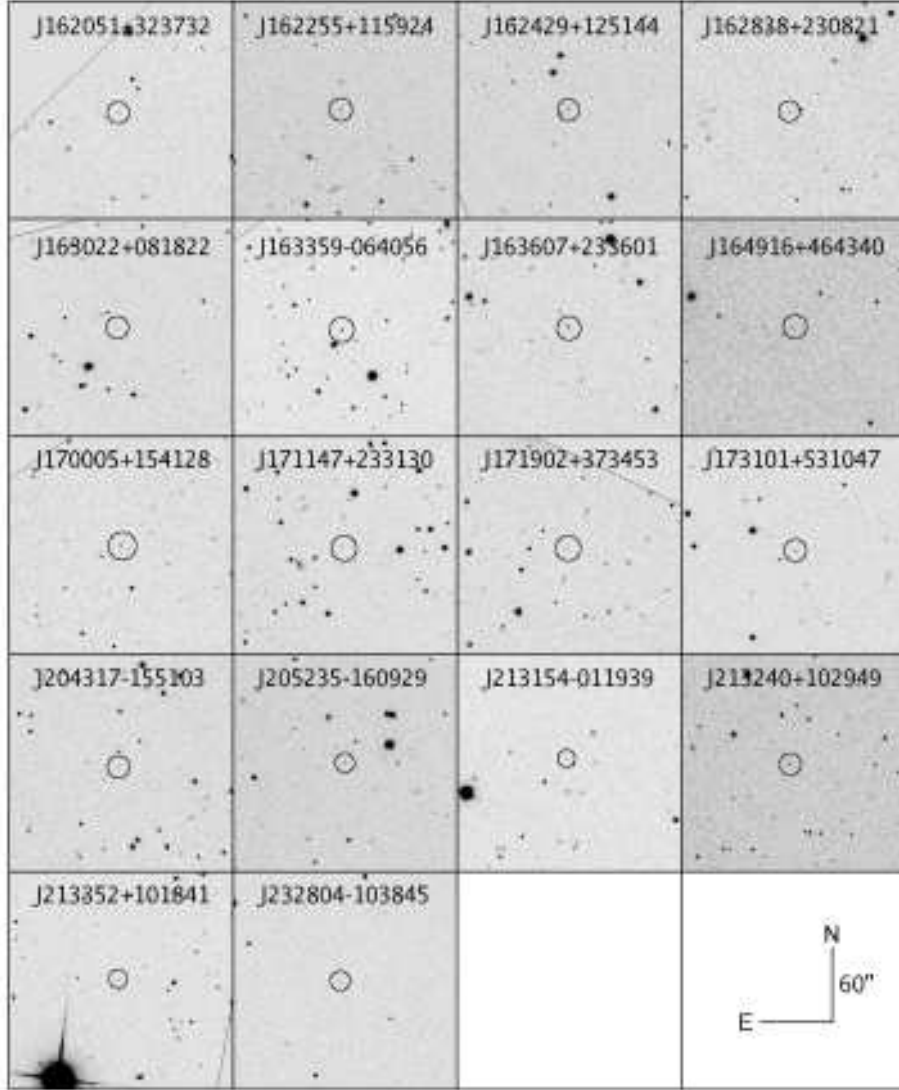


FIG. 1.— (continued) SDSS z finding charts for the 73 new M, L, and T dwarfs found in this work. North is up, East is left. The fields of view are $3' \times 3'$. (Full resolution versions of these finding charts will appear in the published journal edition.)

SDSS i -band 5σ detection limit is 22.5, the SDSS photometric pipeline yields asinh magnitudes below this flux limit (Lupton et al. 1999). For this reason, we identify with brackets those SDSS i magnitudes in Table 1 that imply non-detections. The SDSS designations contain the J2000.0 right ascensions and declinations in sexagesimal format, truncated to the significant digit shown. The positions are accurate to better than $0''.1$ in each coordinate. For brevity, we hereafter refer to the dwarfs by the abbreviated form, SDSS JHHMM \pm DDMM. One T dwarf, SDSS J1534+1615AB, has recently been resolved into a close binary using the laser guide star and adaptive optics systems at the Keck Observatory (Liu et al. 2006). Figure 1 displays $3' \times 3'$ z -band finding charts for the 73 dwarfs in our sample.

Table 2 lists MKO JHK magnitudes for three 2MASS dwarfs (2MASS J0034+0523, 2MASS J1209–1004, 2MASS J2101+1756) as well as UFTI Z magnitudes

may differ from those published here due to reprocessing of the data.

for 2MASS J1209–1004 and seven previously published SDSS L and T dwarfs (Burgasser et al. 2004a; K04). The Z -band data are not used in this analysis but are presented for future reference.

2.3. Spectroscopic Observations

We obtained near-infrared spectra of 65 newly identified SDSS dwarfs whose near-infrared colors are consistent with types mid-L and later. We also obtained spectra of the T dwarf 2MASS J1209–1004 (Burgasser et al. 2004a), the mid-L dwarf 2MASS J2101+1756 (Kirkpatrick et al. 2000), three L dwarfs identified by K04 on the basis of their colors (SDSS J0740+2009, SDSS J0756+2314, and SDSS J0809+4434), one L dwarf with uncertain spectral type (SDSS J0805+4812; K04), and one T dwarf with incomplete spectral coverage (SDSS J2124+0100; K04). The new spectra allow more accurate classification of these previously reported L and T dwarfs. We did not obtain spectra of the two M dwarfs and six early- to mid-L dwarfs because of observing time

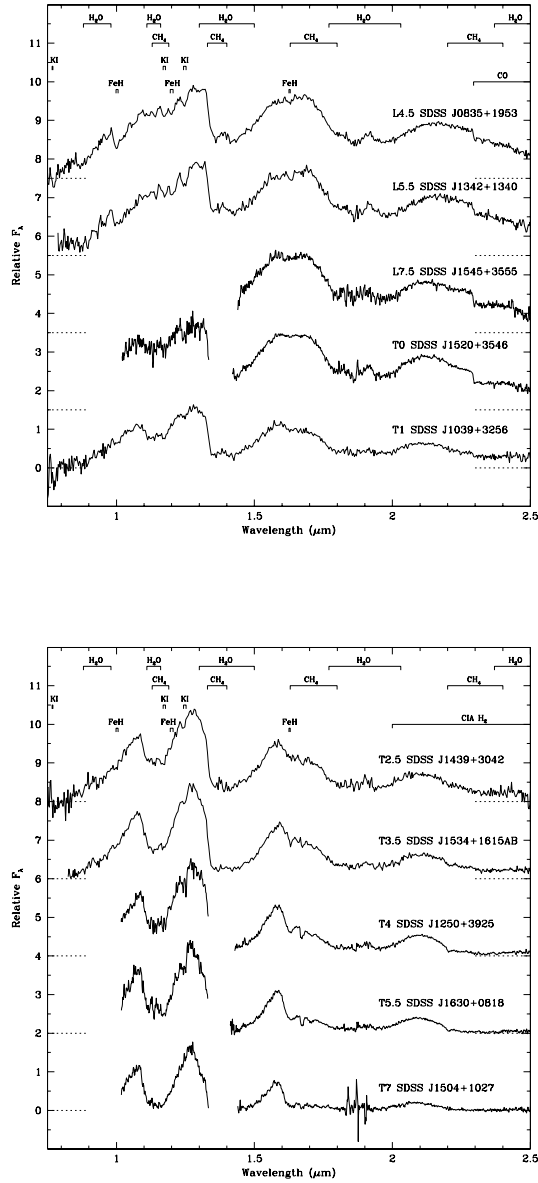


FIG. 2.— Representative optical and near-infrared spectra of the L and T dwarfs discovered in this work. The typical spectral resolution is ~ 150 . SDSS designations are given above the dashed line corresponding to the zero flux level. The locations of significant spectral features are indicated at the top of each panel.

constraints.

The spectra were obtained using the UKIRT Imager/Spectrometer (UIST; Ramsay-Howat et al. 2000) and Cooled Grating Spectrometer (CGS4; Wright et al. 1993) on UKIRT, as well as SpeX at the IRTF. The UKIRT instrument configurations and observational procedures are described by K04. SpeX was used in the low-resolution prism mode with a slit width of $0''.5$, giving a wavelength coverage of 0.8 – 2.5 μm with a resolution of ~ 150 . The on-target exposure time was 120 s, and each star was nodded along the slit for a total observation time of 48–80 min. Flat fields and arc spectra for wavelength calibration were obtained using the SpeX

calibration box lamps. A0 stars were observed as telluric calibrators, and the data were reduced using the SpeXtool package (Cushing et al. 2004). The flux calibration of the spectra was improved by adjusting the relative flux level to match our JHK photometry. Tables 3 and 4 list the instruments and dates of observation for each dwarf in our spectral sample.

Figure 2 shows spectra of selected L and T dwarfs representing the range of types in our sample.⁸ Most spectra cover the wavelength range ~ 1 – 2.5 μm . Interesting and diagnostic absorption features are identified above the displayed spectra.

3. SPECTRAL CLASSIFICATION

The near-infrared classification of L and T dwarfs is generally accomplished either by directly comparing the spectra with standard-dwarf templates or by measuring indices defined for their diagnostic spectral bands (i.e., H_2O and CH_4). As in our past work, we use the spectral-index approach, which is robust even with medium to low signal-to-noise ratios and spectral resolution.

To place our present sample of SDSS L dwarfs in the context of those presented by G02 and K04, we classified the L dwarfs using the near-infrared spectral indices of G02. However, we classified the T dwarfs using the new spectral indices of Burgasser et al. (2005), which unify the similar T classification schemes of G02 and Burgasser et al. (2002a). The unified scheme uses five primary indices: $\text{H}_2\text{O}-J$ centered at 1.15 μm , CH_4-J at 1.32 μm , $\text{H}_2\text{O}-H$ at 1.4 μm , CH_4-H at 1.65 μm , and CH_4-K at 2.2 μm . The values of the unified indices are inverted with respect to those of G02, i.e., the values of the unified indices decrease with later T type. We used both the G02 and unified indices to classify the suspected L–T transition dwarfs, as in some cases one scheme suggests a late-L type and the other scheme suggests an early-T type.

Table 3 lists the G02 indices of 61 L and early-T dwarfs for which we have obtained new near-infrared spectra. Of these, 56 are newly identified from the SDSS and 5 are previously known SDSS and 2MASS dwarfs, as described in §2.3. Values in square brackets are uncertain and have not been included in the final spectral classification. When only a single index could be measured reliably, the spectra were visually compared with standard subtypes for more accurate classification. Table 4 lists the indices for 45 late-L and T dwarfs from the unified scheme of Burgasser et al. (2005).⁹ In both tables, the uncertainty in the mean spectral type is ± 0.5 subtype, unless otherwise stated.

Table 5 lists, in order of spectral type, the optical and/or near-infrared colors of the 72 dwarfs for which we have new spectra, plus 2MASS J0034+0523. Multiple photometric and spectroscopic measurements (including data from K04) were averaged before determining the final colors and types. The $i-z$ colors for dwarfs not detected in i were computed using the SDSS 5σ detection limit of $i = 22.5$. The spectral types of all newly dis-

⁸ More extensive spectral and photometric data for this and other samples may be found at <http://www.jach.hawaii.edu/~skl/LTdata.html>

⁹ Revised spectral types for previously published SDSS T dwarfs and two late-L dwarfs (SDSS J1104+5548 and SDSS J2047–0718) are given in Table 14 of Burgasser et al. (2005).

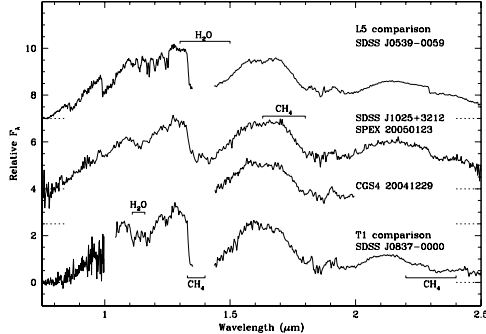


FIG. 3.— The unusual spectra of the $L7.5 \pm 2.5$ dwarf, SDSS J1025+3212 (thick lines). The spectra show $1.1 \mu\text{m}$ H_2O and 1.4 , $2.2 \mu\text{m}$ CH_4 absorption features usually associated with T0 dwarfs, as well as H_2O features typical of L5 dwarfs. The $1.6 \mu\text{m}$ CH_4 absorption features seen in the CGS4 and SpeX spectra appear variable. Spectra of SDSS J0539–0059 (L5) and SDSS J0837–0000 (T1) are shown for reference (Leggett et al. 2000).

covered L and T dwarfs are taken from Tables 3 and 4, respectively. The subtypes adopted for the L8–T1 dwarfs are those produced by the classification scheme that exhibited the more definitive and complete set of indices for its resultant subtype. If both schemes indicated a late-L type, then the G02 designation was adopted. If both schemes indicated an early-T type, then the unified T classification of Burgasser et al. (2005) was used. The only exception to these rules is SDSS J1511+0607 (T0 ± 2), for which a definitive set of indices was derived only in the G02 scheme. The uncertainties of all the subtypes listed in Table 5 are ± 0.5 subtype, unless otherwise stated.

The uncertainties of the L6–T1 dwarfs are typically > 1 subtype, which suggests that the presence of condensate cloud decks undermines the internal consistency of the spectral indices. Consequently, the indices become more a probe of cloud optical depth than a measure of effective temperature (Stephens 2003, K04, Leggett et al. 2005). Approximately 75% of the dwarfs whose mean spectral types are very uncertain have CH_4 - K spectral types that are significantly earlier than indicated by their J - and H -band indices. This effect is also seen in the L8–T0 sample of K04. Because the optical and K -band fluxes emerge from more opaque regions of the atmosphere (specifically from regions above the cloud decks), they are likely to be better indicators of T_{eff} than the flux emerging from the clear J - and H -band windows. Golimowski et al. (2004a) showed that T_{eff} is approximately constant for L7 to T4 types, so it might be expected that the L–T transition dwarfs have a constant optical and K -band spectral type of $\sim L8$, while their J - and H -band indices reflect changes in optical depth caused by varying condensate clouds.

The newly identified L dwarf SDSS J1025+3212 ($L7.5 \pm 2.5$) has particularly scattered spectral indices (Tables 3 and 4), indicating that it may be multiple and/or variable. Figure 3 shows the SpeX and CGS4 spectra of SDSS J1025+3212 along with comparison L5 and T1 spectra. Its H_2O - J index suggests a T0 type, while its CH_4 - J , H_2O - H , and CH_4 - K indices suggest a

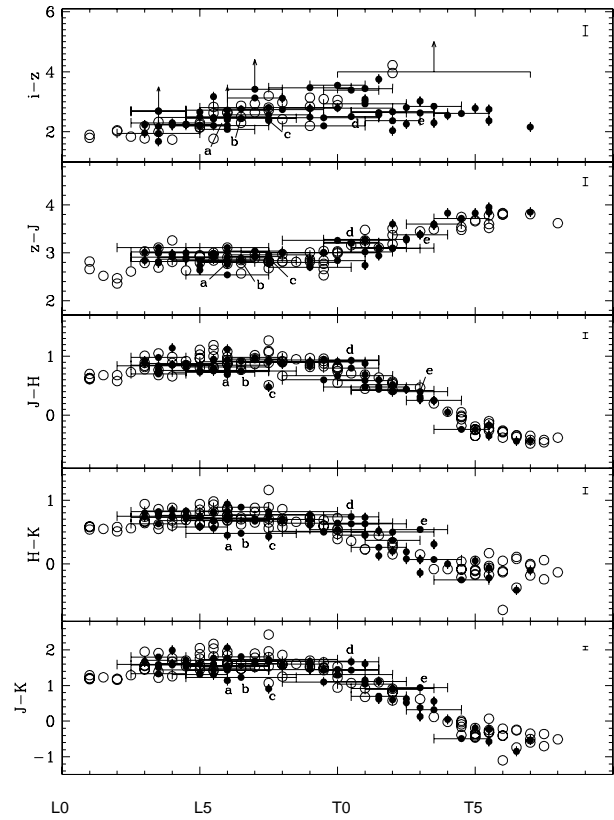


FIG. 4.— Optical and near-infrared colors of the dwarfs listed in Table 5 of this work (solid points) and reported previously by Knapp et al. (2004) and Leggett et al. (2002) (open circles). Five dwarfs with unusual colors are labelled, as discussed in §4: (a) SDSS J1033+4005, (b) SDSS J1422+2215, (c) SDSS J1121+4332, (d) SDSS J1516+3053, and (e) SDSS J1415+5724. Horizontal error bars are shown for those dwarfs whose spectral types are more uncertain than ± 0.5 subtype. The small vertical error bar in the upper-rightmost corner of each panel indicates the typical color error. In the top panel, the i - z colors of dwarfs not detected in SDSS i are shown with arrows as lower limits based on a 5σ detection limit of $i = 22.5$. Dwarfs with type $> T0$ are almost all non-detections in SDSS i , shown by the large barred arrow in i - z .

mid-L type. Evidence of CH_4 absorption at $1.6 \mu\text{m}$ is seen in the CGS4 spectrum but not in the SpeX spectrum obtained one month later. Attempts to reproduce the spectrum as a composite of L and T spectra failed. High-resolution imaging and photometric monitoring are needed to investigate the nature of this peculiar brown dwarf.

Ambiguous types like SDSS J1025+3212 give cause for reexamining the near-infrared classification scheme for L dwarfs, especially near the L–T transition. Moreover, two of the first known early-T dwarfs, SDSS J0423-0414 and SDSS J1021-0304, have recently been found to be binary (Burgasser et al. 2006; Burgasser et al., in prep.). These binary dwarfs contributed significantly to the definition of G02’s standard indices at the L–T transition. Revision of these indices must be based on single dwarfs, so knowing which transition dwarfs are multiple

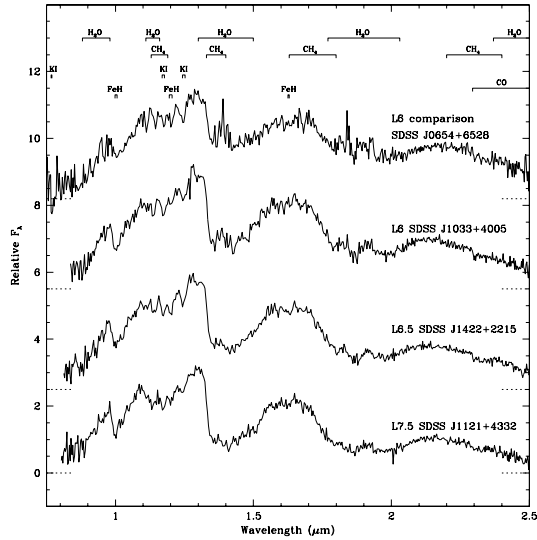


FIG. 5.— Spectra of unusually blue L dwarfs with strong H₂O and FeH absorption bands. These features may be due to subsolar metallicity and/or thinner condensate cloud decks. A spectrum of the typical L6 dwarf SDSS J0654+6528 is shown for reference.

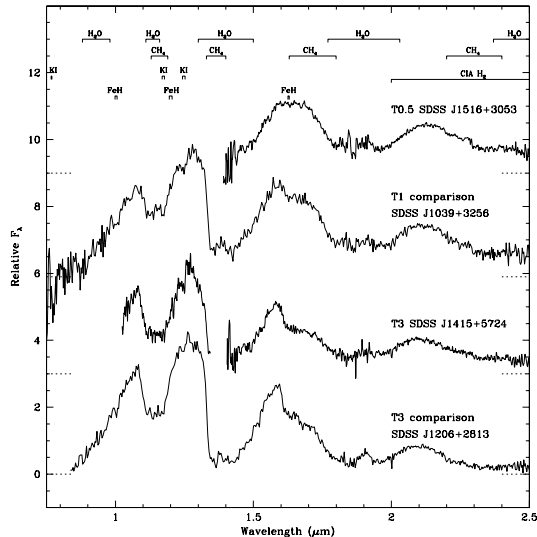


FIG. 6.— Spectra of unusually red early T dwarfs (thick curves) compared with spectra of typical T dwarfs. SDSS J1516+3053 has weak methane bands, but strong water bands. SDSS J1415+5724 has unusually weak K-band methane.

is prerequisite to merging a revised L infrared classification scheme with the unified T classification scheme of Burgasser et al. (2005). Several high-resolution imaging searches for close-binary brown dwarfs are being conducted with the *Hubble Space Telescope* and ground-based adaptive optics imagers (Burgasser et al. 2003; Bouy et al. 2003; McCaughrean et al. 2004; Goliowski et al. 2004b; Liu & Leggett 2005; Liu et al. 2006; Burgasser et al. 2006). Segregating the single and multiple transition dwarfs will not only help de-

fine the “standard” L and T sequences, but it will clarify our understanding of the breakup of the condensate cloud decks across the L–T transition, which is presently a controversial aspect of ultracool atmosphere models (Burgasser et al. 2002b; Tsuji & Nakajima 2003; K04, Burrows et al. 2005).

4. SPECTRAL TYPE AND NEAR-INFRARED COLORS

Figure 4 shows plots of SDSS and MKO colors versus spectral type for the L and T dwarfs listed in Table 5 of this paper and in Table 9 of K04. Most of the spectral types have been assigned by us from our own spectra, but a few types are adopted from other published work. (See notes for Table 5 and K04’s Table 9.) While the colors are generally correlated with spectral type, they are also significantly scattered. The $J-H$ colors of L3–T1 dwarfs show a dispersion of ~ 0.5 mag, as do the $H-K$ colors of all dwarfs later than type L3. These dispersions are likely due to wide ranges of grain sedimentation properties and metallicity in the L dwarfs and wide ranges of gravity and metallicity in the T dwarfs (K04, and references therein).

As noted by K04, a small population of L dwarfs has unusually blue near-infrared colors, and we have found in this sample a small population of T dwarfs with unusually red colors. These unusual dwarfs are marked in Figure 4. Figure 5 shows the spectra of the anomalously blue mid-L dwarfs SDSS J1033+4005, SDSS J1422+2215 and SDSS J1121+4332, along with the spectrum of the normal L6 dwarf SDSS J0654+6528. The spectra of the blue dwarfs show strong H₂O and FeH absorption bands, which may be due to subsolar metallicity and/or thinner condensate cloud decks. Figure 6 shows the spectra of the unusually red early-T dwarfs SDSS J1516+3053 and SDSS J1415+5724, along with two normal reference spectra. SDSS J1516+3053 shows weak CH₄ bands but strong H₂O bands. SDSS J1415+5724 shows an unusually weak K-band CH₄ band. Attempts to reproduce these spectra as composite binary systems failed, but, as previously discussed, we may not know the true spectra of single L–T transition dwarfs. Liu et al. (2006) show that one of our new T dwarfs, SDSS J1534+1615, is a close T1-T2 and T5-T6 binary whose brighter J -band component is the fainter one in H and K . This near-infrared flux inversion suggests that the system straddles the “early T hump” in the absolute magnitude-color diagrams (e.g. K04, Goliowski et al. 2004). Clearly, high-resolution imaging of dwarfs with unusual colors is warranted, as are parallax and velocity studies to determine their kinematic properties.

5. SUMMARY

Thanks to the great gains in detection efficiency provided by large digital sky surveys, observers have reached the once-unimaginable position of routinely discovering nearby field brown dwarfs. In this paper, we report the discovery of 71 L and T dwarfs identified during our ongoing search for high-redshift quasars and brown dwarfs in SDSS imaging data. Using near-infrared photometry and spectra obtained over the past two years at UKIRT and IRTF, we have classified these dwarfs using the L classification scheme of Geballe et al. (2002) and the new unified T classification scheme of Burgasser et al. (2005). The near-infrared colors of the 71 dwarfs exhibit the same trends, scatter, and anomalies noted in previously re-

ported samples. The unusual spectral features exhibited by some dwarfs may lead to a better understanding of their underlying atmospheric properties. We plan to apply our results to the revision of the spectral infrared indices used in the near-infrared classification of L dwarfs. We will also integrate the 71 new L and T into a complete magnitude-limited catalog for the purpose of determining the substellar luminosity function.

6. ACKNOWLEDGEMENTS

We thank the staff at APO, IRTF, and UKIRT for their assistance with the observations and data acquisition. Some data were obtained through the UKIRT Service Programme. UKIRT is operated by the Joint Astronomy Centre on behalf of the U.K. Particle Physics and Astronomy Research Council. APO is owned and operated by the Astrophysical Research Consortium (ARC). The IRTF is operated by the University of Hawaii under Cooperative Agreement no. NCC 5-538 with the National Aeronautics and Space Administration (NASA), Office of Space Science, Planetary Astronomy Program. This publication makes use of data products from the Two Micron All Sky Survey, which is a joint project of the University of Massachusetts and the Infrared Processing and Analysis Center (IPAC)/California Institute of Technology, funded by NASA and the National Science Foundation. This research has also made use of the NASA/IPAC Infrared Science Archive, which is operated

by the Jet Propulsion Laboratory, California Institute of Technology, under contract with NASA.

XF acknowledges support from NSF grant AST 03-07384, a Sloan Research Fellowship and a David and Lucile Packard Fellowship. TRG's research is supported by the Gemini Observatory, which is operated by the Association of Universities for Research in Astronomy on behalf of the international Gemini partnership of Argentina, Australia, Brazil, Canada, Chile, the United Kingdom, and the United States of America.

The Sloan Digital Sky Survey (SDSS) is managed by ARC for the Participating Institutions: The University of Chicago, Fermilab, the Institute for Advanced Study, the Japan Participation Group, The Johns Hopkins University, the Korean Scientist Group, Los Alamos National Laboratory, the Max-Planck-Institute for Astronomy, the Max-Planck-Institute for Astrophysics, New Mexico State University, University of Pittsburgh, University of Portsmouth, Princeton University, the United States Naval Observatory, and the University of Washington. Funding for SDSS has been provided by the Alfred P. Sloan Foundation, the Participating Institutions, the National Aeronautics and Space Administration, the National Science Foundation, the U.S. Department of Energy, the Japanese Monbukagakusho, and the Max Planck Society. The SDSS Web site is <http://www.sdss.org/>.

REFERENCES

Abazajian, K., et al. 2004, AJ, 128, 502
 Allen, P. R., Koerner, D. W., Reid, I. N., & Trilling, D. E. 2005, ApJ, 625, 385
 Bouy, H., Brandner, W., Martín, E. L., Delfosse, X., Allard, F., & Basri, G. 2003, AJ, 126, 1526
 Burgasser, A.J. 2004b, ApJS, 155, 191
 Burgasser, A. J., et al. 1999, ApJ, 522, L65
 Burgasser, A. J., Geballe, T. R., Leggett, S. K., Kirkpatrick, J. D., & Goliowski, D. A. 2005, ApJ, in press
 Burgasser, A. J., Kirkpatrick, J. D., Brown, M. E., Reid, I. N., Burrows, A., Liebert, J., Matthews, K., Gizis, J. E., Dahn, C. C., Monet, D. G., Cutri, R. M., & Skrutskie, M. F. 2002a, ApJ, 564, 421
 Burgasser, A. J., Kirkpatrick, J. D., Reid, I. N., Brown, M. E., Miskey, C. L., & Gizis, J. E. 2003, ApJ, 586, 512
 Burgasser, A. J., Marley, M. S., Ackerman, A. S., Saumon, D., Lodders, K., Dahn, C. C., Harris, H. C., & Kirkpatrick, J. D. 2002b, ApJ, 571, L151
 Burgasser, A. J., McElwain, M. W., Kirkpatrick, J. D., Cruz, K. L., Tinney, C. G., & Reid, I. N. 2004a, AJ, 127, 2856
 Burgasser, A. J., Reid, I. N., Leggett, S. K., Kirkpatrick, J. D., Liebert, J., Burrows, A. 2006, ApJ, in press
 Burrows, A., Sudarsky, D., Hubeny, I. 2005, astro-ph/0509066
 Cushing, M. C., Vacca, W. D., & Rayner, J. T. 2004, PASP, 116, 362
 Epchtein, N. 1997, in The Impact of Large Scale Near-IR Sky Surveys, ed. F. Garzón, N. Epchtein, A. Omont, W. B. Burton, and P. Persei (Dordrecht: Kluwer), 15
 Fan, X., et al. 1999, AJ, 118, 1
 Fan, X., et al. 2000a, AJ, 120, 1167
 Fan, X., et al. 2000b, AJ, 119, 928
 Fan, X., et al. 2001a, AJ, 122, 2833
 Fan, X., et al. 2001b, AJ, 121, 54
 Fan, X., et al. 2003, AJ, 125, 1649
 Fan, X., et al. 2004, AJ, 128, 515
 Fukugita, M., Ichikawa, T., Gunn, J.E., Doi, M., Shimasaku, K., & Schneider, D.P. 1996, AJ, 111, 1748
 Geballe, T. R., et al. 2002, ApJ, 564, 466 (G02)
 Goliowski, D. A., et al. 2004a, AJ, 127, 3516
 Goliowski, D. A., et al. 2004b, AJ, 128, 1733
 Gunn, J.E., et al. 1998, AJ, 116, 3040
 Hawarden, T. G., Leggett, S. K., Letawsky, M. B., Ballantyne, D. R., & Casali, M. M. 2001, MNRAS, 325, 563
 Hawley, S., et al. 2002, AJ, 123, 3409
 Hogg, D.W., Finkbeiner, D.P., Schlegel, D.J., & Gunn, J.E. 2001, AJ, 122, 2129
 Kirkpatrick, J. D. 2005, ARA&A, 43, 195
 Kirkpatrick, J. D., Reid, I. N., Liebert, J., Cutri, R. M., Nelson, B., Beichman, C. A., Dahn, C. C., Monet, D. G., Gizis, J. E., & Skrutskie, M. F. 1999, ApJ, 519, 802
 Kirkpatrick, J. D., Reid, I. N., Liebert, J., Gizis, J. E., Burgasser, A. J., Monet, D. G., Dahn, C. C., Nelson, B., & Williams, R. J. 2000, AJ, 120, 447
 Knapp, G.R., et al. AJ, 2004, 127, 3553 (K04)
 Leggett, S. K., et al. 2000, ApJ, 536, L35
 Leggett, S. K., et al. 2002, ApJ, 2002, 564, 452
 Leggett, S. K., Allard, F., Burgasser, A. J., Jones, H. R. A., Marley, M. S., & Tsuji, T. 2005, in Proceedings of the 13th Cool Stars Workshop, ESA Special Publications Series, in press.
 Liu, M. C., & Leggett, S. K. 2005, ApJ, 634, 616
 Liu, M. C., Leggett, S. K., Goliowski, D. A., Chiu, K., Fan, X., Geballe, T. R., Schneider, D. P., Brinkman, J. 2006, ApJ, submitted
 Lupton, R. H., Gunn, J. E., & Szalay, A. S. 1999, AJ, 118, 1406
 McCaughrean, M. J., Close, L. M., Scholz, R.-D., Lenzen, R., Biller, B., Brandner, W., Hartung, M., & Lodieu, N. 2004, A&A, 413, 1029
 Oke, J.B., & Gunn, J.E. 1983, ApJ, 266, 713
 Pier, J.R., Munn, J.A., Hindsley, R.B., Hennessy, G.S., Kent, S.M., Lupton, R.H., & Ivezic, Z. 2003, AJ, 125, 1559
 Ramsay-Howat, S. K., Ellis, M. A., Gostick, D. C., Hastings, P. R., Strachan, M., & Wells, M. 2000, Proc. SPIE, 4008, 1067
 Rayner, J. T., Toomey, D. W., Onaka, P. M., Denault, A. J., Stahlberger, W. E., Vacca, W. D., Cushing, M. C., & Wang, S. PASP, 115, 362
 Richards, G.T., et al. 2002, AJ, 123, 2945
 Roche, P. F., Lucas, P. W., MacKay, C. D., Ettedgui-Atad, E., Hastings, P. R., Bridger, A., Rees, N. P., Leggett, S. K., Davis, C., Holmes, A. R., & Handford, T. 2003, Proc. SPIE, 4841, 901
 Schneider, D. P., et al. 2002, AJ, 123, 458
 Simons, D. A., & Tokunaga, A. T. 2002, PASP, 114, 169

Skrutskie, M. F., et al. 1997, in The Impact of Large Scale Near-IR Sky Surveys, ed. F. Garzón, N. Epcstein, A. Omont, B. Burton, and P. Persei (Dordrecht: Kluwer), 25

Smith, J., et al. 2002, AJ, 123, 2121

Stephens, D. C. 2003, in IAY Symp. 211, Brown Dwarfs, ed. E. Martín (San Francisco: ASP), 355

Stoughton, C., et al. 2002, AJ, 123, 485

Strauss, M. A., et al. 1999, ApJ, 522, L61

Tokunaga, A. T., Simons, D. A., & Vacca, W. D. 2002, PASP, 114, 180

Tsuji, T., & Nakajima, T. 2003, ApJ, 585, L151

Tsvetanov, Z. I., et al. 2000, ApJ, 531, L61

Wright, G. S., Mountain, C. M., Bridger, A., Daly, P. N., Griffin, J. L., & Ramsay-Howat, S. K. 1993, Proc. SPIE, 1946, 547

York, D. G., et al. 2000, AJ, 120, 1579

Zheng, W., et al. 2000, AJ, 120, 1607

TABLE 1
NEW M, L, AND T DWARF PHOTOMETRY

SDSS Name	SDSS <i>i</i> ^a (AB)	SDSS <i>z</i> (AB)	SDSS Run	UT Date (yyyymmdd)	MKO <i>J</i> (Vega)	MKO <i>H</i> (Vega)	MKO <i>K</i> (Vega)	Instrument	UT Date (yyyymmdd)
J000250.98+245413.8	22.20 ± 0.16	19.99 ± 0.08	4851	20040923	17.02 ± 0.03	16.09 ± 0.03	15.42 ± 0.03	UFTI	20050727
J003609.26+241343.3	[22.97 ± 0.39]	20.07 ± 0.11	4836	20040917	17.08 ± 0.05	16.28 ± 0.03	15.48 ± 0.03	UFTI	20050727
J011912.22+240331.6	[24.07 ± 0.49]	20.46 ± 0.11	4829	20040915	16.86 ± 0.03	16.46 ± 0.03	16.26 ± 0.03	SpeX	20050811
J020608.97+223559.2	22.42 ± 0.17	19.25 ± 0.04	4844	20040921	16.40 ± 0.05	15.56 ± 0.05	15.03 ± 0.05	UFTI	20050208
J020608.97+223559.2	22.42 ± 0.17	19.25 ± 0.04	4844	20040921	16.31 ± 0.03	15.62 ± 0.03	15.05 ± 0.03	SpeX	20050812
J024256.98+212319.6	22.24 ± 0.18	20.02 ± 0.09	4844	20040921	17.05 ± 0.03	16.19 ± 0.03	15.43 ± 0.03	SpeX	20051107
J024749.90-163112.6	[23.24 ± 0.39]	19.83 ± 0.11	5069	20041215	16.73 ± 0.03	16.31 ± 0.03	15.81 ± 0.03	SpeX	20050812
J032553.17+042540.1	[23.59 ± 0.57]	19.75 ± 0.08	5065	20041214	15.88 ± 0.03	16.24 ± 0.03	16.48 ± 0.03	SpeX	20050811
J032553.17+042540.1	[23.59 ± 0.57]	19.75 ± 0.08	5065	20041214	15.92 ± 0.03	16.26 ± 0.03	16.45 ± 0.05	SpeX	20050812
J035104.37+481046.8	[22.84 ± 0.30]	19.57 ± 0.06	4887	20041015	16.33 ± 0.05	15.80 ± 0.05	15.15 ± 0.05	UFTI	20050208
J035104.37+481046.8	[22.84 ± 0.30]	19.57 ± 0.06	4887	20041015	16.27 ± 0.03	15.81 ± 0.03	15.20 ± 0.03	SpeX	20050812
J065405.63+652805.4	20.97 ± 0.05	18.89 ± 0.04	5060	20041213	16.08 ± 0.03	15.35 ± 0.03	14.59 ± 0.03	SpeX	20050121
J073922.26+661503.5	[23.90 ± 0.33]	19.86 ± 0.08	4887	20041015	16.75 ± 0.03	16.31 ± 0.03	16.05 ± 0.03	SpeX	20050407
J082030.12+103737.0	[22.75 ± 0.25]	20.03 ± 0.09	5194	20050312	17.03 ± 0.03	16.09 ± 0.05	15.58 ± 0.03	SpeX	20050407
J083506.16+195304.4	21.10 ± 0.07	18.84 ± 0.05	5045	20041212	15.94 ± 0.03	15.12 ± 0.03	14.41 ± 0.03	SpeX	20050121
J085116.20+181730.0	21.92 ± 0.15	19.68 ± 0.08	5061	20041213	16.68 ± 0.03	15.80 ± 0.04	14.97 ± 0.03	SpeX	20050121
J085834.42+325627.7	22.09 ± 0.15	19.07 ± 0.05	3606	20030125	16.33 ± 0.03	15.45 ± 0.03	14.72 ± 0.03	UFTI	20040114
J090900.73+652527.2	[23.46 ± 0.38]	18.75 ± 0.05	4264	20031120	15.81 ± 0.03	15.32 ± 0.03	15.19 ± 0.03	SpeX	20050121
J100711.74+193056.2	[22.93 ± 0.29]	19.76 ± 0.09	5183	20050310	16.75 ± 0.05	15.85 ± 0.05	15.15 ± 0.03	SpeX	20050407
J102552.43+321234.0	[22.67 ± 0.30]	19.69 ± 0.08	4576	20040416	16.89 ± 0.05	15.98 ± 0.03	15.16 ± 0.03	UFTI	20040626
J102751.48+400931.7 ^b	22.14 ± 0.16	19.98 ± 0.08	3818	20030326	17.10 ± 0.05	16.49 ± 0.03	15.87 ± 0.03	UFTI	20040118
J103321.92+400549.5	21.94 ± 0.16	19.54 ± 0.06	3647	20030201	16.74 ± 0.03	16.05 ± 0.04	15.60 ± 0.05	SpeX	20050121
J103931.35+325625.5	[22.78 ± 0.31]	19.41 ± 0.06	4576	20040416	16.16 ± 0.03	15.47 ± 0.03	15.01 ± 0.03	UFTI	20041229
J104335.08+121314.1	21.99 ± 0.19	18.86 ± 0.04	3836	20030331	15.82 ± 0.03	14.87 ± 0.03	14.20 ± 0.03	UFTI	20040118
J104829.21+091937.8	[24.31 ± 0.60]	19.69 ± 0.08	3031	20020312	16.39 ± 0.03	15.95 ± 0.03	15.87 ± 0.03	UFTI	20040118
J105213.51+442255.7	[22.94 ± 0.40]	19.11 ± 0.06	3530	20021213	15.89 ± 0.03	15.09 ± 0.03	14.46 ± 0.03	UFTI	20040118
J111320.16+343057.9	21.99 ± 0.14	19.76 ± 0.07	4550	20040413	16.92 ± 0.03	16.00 ± 0.03	15.26 ± 0.03	UFTI	20040626
J112118.57+433246.5	22.31 ± 0.19	19.93 ± 0.09	3813	20030324	17.04 ± 0.05	16.56 ± 0.04	16.13 ± 0.04	SpeX	20050121
J114220.63+114440.3 ^b	22.46 ± 0.25	20.24 ± 0.11	3836	20030331	17.89 ± 0.06	17.40 ± 0.05	16.84 ± 0.09	UFTI	20040626
J120602.51+281328.7	[24.11 ± 0.85]	19.48 ± 0.07	5112	20050117	16.10 ± 0.03	15.83 ± 0.03	15.97 ± 0.03	UFTI	20050305
J121440.95+631643.4	[24.90 ± 0.78]	19.65 ± 0.10	2304	20010518	16.05 ± 0.03	15.80 ± 0.03	15.73 ± 0.04	SpeX	20050121
J121659.17+300306.3	22.41 ± 0.24	19.71 ± 0.10	5061	20041213	16.89 ± 0.05	16.19 ± 0.03	15.56 ± 0.03	SpeX	20050407
J121951.45+312849.4	21.97 ± 0.15	18.85 ± 0.04	4599	20040425	15.85 ± 0.03	14.98 ± 0.03	14.30 ± 0.03	UFTI	20040626
J123330.63+423948.8 ^c	[22.79 ± 0.27]	19.92 ± 0.09	3840	20030401	17.24 ± 0.03	16.33 ± 0.03	15.65 ± 0.03	UFTI	20040118
J125011.65+392553.9	[23.78 ± 0.48]	19.95 ± 0.09	3900	20030426	16.12 ± 0.03	16.07 ± 0.03	16.07 ± 0.03	UFTI	20040118
J134203.11+134022.2	22.31 ± 0.20	19.86 ± 0.09	3971	20030530	16.90 ± 0.03	15.95 ± 0.03	15.13 ± 0.03	UFTI	20040626
J134403.84+083950.9 ^d	[23.09 ± 0.31]	19.98 ± 0.08	3909	20030428	17.22 ± 0.03	16.45 ± 0.03	15.98 ± 0.03	UFTI	20040120
J134525.57+521634.0	22.02 ± 0.17	19.84 ± 0.10	3177	20020508	17.05 ± 0.03	16.30 ± 0.03	15.54 ± 0.03	SpeX	20050407
J135852.68+374711.9	[25.34 ± 0.45]	19.89 ± 0.08	3900	20030426	16.17 ± 0.03	16.41 ± 0.03	16.66 ± 0.05	UFTI	20040118
J140023.12+433822.3	[22.52 ± 0.20]	19.08 ± 0.04	3716	20030311	16.16 ± 0.03	15.18 ± 0.03	14.47 ± 0.03	UFTI	20040118
J140255.66+080055.2	[22.87 ± 0.31]	19.93 ± 0.08	3903	20030427	16.85 ± 0.03	16.25 ± 0.03	15.73 ± 0.03	UFTI	20040120
J141530.05+572428.7	[22.56 ± 0.30]	19.87 ± 0.09	3225	20020609	16.49 ± 0.03	16.09 ± 0.03	15.55 ± 0.03	UFTI	20040210
J141659.78+500626.4	22.18 ± 0.23	19.70 ± 0.10	3177	20020508	16.81 ± 0.03	16.04 ± 0.03	15.35 ± 0.03	UFTI	20040214
J141659.78+500626.4	22.18 ± 0.23	19.70 ± 0.10	3177	20020508	16.76 ± 0.05	16.01 ± 0.03	15.35 ± 0.03	SpeX	20050407
J142227.25+221557.1	22.16 ± 0.14	19.71 ± 0.09	4678	20040614	16.87 ± 0.03	16.12 ± 0.03	15.64 ± 0.03	UFTI	20050306

TABLE 1 — *Continued*

SDSS Name	SDSS <i>i</i> ^a (AB)	SDSS <i>z</i> (AB)	SDSS Run	UT Date (yyymmdd)	MKO <i>J</i> (Vega)	MKO <i>H</i> (Vega)	MKO <i>K</i> (Vega)	Instrument	UT Date (yyymmdd)
J143553.25+112948.6	[23.40 ± 0.44]	20.13 ± 0.10	3996	20030622	17.04 ± 0.03	16.52 ± 0.04	16.15 ± 0.06	UFTI	20040626
J143945.86+304220.6	[23.64 ± 0.49]	20.24 ± 0.10	4570	20040415	16.97 ± 0.03	16.53 ± 0.03	16.34 ± 0.05	UFTI	20040626
J144128.52+504600.4	21.83 ± 0.15	19.87 ± 0.08	3180	20020508	16.86 ± 0.03	15.98 ± 0.03	15.18 ± 0.03	UFTI	20040214
J150411.63+102718.4	[24.66 ± 0.78]	20.34 ± 0.14	3894	20030425	16.49 ± 0.03	16.92 ± 0.03	17.02 ± 0.03	UFTI	20040120
J151114.66+060742.9	21.88 ± 0.19	19.09 ± 0.06	2391	20010616	15.83 ± 0.03	15.16 ± 0.03	14.52 ± 0.03	UFTI	20050306
J151506.11+443648.3	22.07 ± 0.15	19.50 ± 0.06	3180	20020508	16.54 ± 0.03	15.63 ± 0.03	14.86 ± 0.03	UFTI	20040211
J151643.01+305344.4	[23.18 ± 0.35]	19.99 ± 0.11	4002	20030623	16.79 ± 0.03	15.86 ± 0.03	15.12 ± 0.03	UFTI	20040211
J152039.82+354619.8	21.86 ± 0.12	18.31 ± 0.03	3818	20030326	15.47 ± 0.03	14.56 ± 0.03	14.02 ± 0.03	UFTI	20040211
J153417.05+161546.1AB	[24.17 ± 0.61]	20.20 ± 0.12	5194	20050312	16.62 ± 0.03	16.37 ± 0.03	16.06 ± 0.03	UFTI	20050305
J153453.33+121949.2	20.48 ± 0.05	18.18 ± 0.03	5317	20050511	15.27 ± 0.03	14.42 ± 0.03	13.69 ± 0.03	SpeX	20050811
J154009.36+374230.3	[22.67 ± 0.26]	19.03 ± 0.06	3965	20030529	16.33 ± 0.03	15.42 ± 0.03	14.65 ± 0.03	UFTI	20040214
J154508.93+355527.3	22.28 ± 0.18	19.87 ± 0.09	3965	20030529	16.97 ± 0.03	16.04 ± 0.03	15.29 ± 0.03	UFTI	20040214
J154849.02+172235.4	21.32 ± 0.08	18.82 ± 0.04	4674	20040613	16.09 ± 0.03	15.24 ± 0.03	14.49 ± 0.03	UFTI	20050305
J161731.65+401859.7	22.09 ± 0.16	19.81 ± 0.10	3226	20020609	16.83 ± 0.03	15.69 ± 0.03	14.84 ± 0.03	SpeX	20050407
J162051.17+323732.1	[23.44 ± 0.48]	20.01 ± 0.11	3964	20030529	17.17 ± 0.04	16.23 ± 0.03	15.40 ± 0.03	UFTI	20040728
J162255.27+115924.1	21.93 ± 0.17	19.43 ± 0.06	5194	20050312	16.89 ± 0.05	16.15 ± 0.03	15.46 ± 0.03	SpeX	20050408
J162429.36+125144.0 ^d	20.79 ± 0.15	18.97 ± 0.05	5323	20050512	16.44 ± 0.03	15.72 ± 0.03	15.18 ± 0.03	UFTI	20050307
J162838.77+230821.1	[24.40 ± 0.58]	20.23 ± 0.10	3927	20030501	16.25 ± 0.03	16.63 ± 0.04	16.72 ± 0.03	UFTI	20040728
J163022.92+081822.0	[23.82 ± 0.61]	20.13 ± 0.10	3996	20030622	16.18 ± 0.03	16.35 ± 0.03	16.41 ± 0.03	UFTI	20040118
J163359.23-064056.5	21.31 ± 0.08	18.76 ± 0.04	5384	20050605	16.00 ± 0.03	15.25 ± 0.03	14.54 ± 0.03	SpeX	20050811
J163607.48+233601.6 ^d	21.82 ± 0.19	19.57 ± 0.06	3997	20030622	16.86 ± 0.03	16.21 ± 0.03	15.61 ± 0.03	UFTI	20040728
J164916.89+464340.0	22.39 ± 0.19	19.73 ± 0.09	4011	20030625	17.09 ± 0.03	16.33 ± 0.03	15.74 ± 0.03	UFTI	20040728
J170005.43+154128.8 ^d	21.53 ± 0.10	19.14 ± 0.05	4014	20030626	16.21 ± 0.03	15.65 ± 0.03	15.12 ± 0.03	UFTI	20040728
J171147.17+233130.5	21.90 ± 0.24	19.95 ± 0.13	3177	20020508	16.84 ± 0.03	16.00 ± 0.03	15.25 ± 0.03	SpeX	20050813
J171902.15+373453.6 ^d	21.87 ± 0.13	20.28 ± 0.11	4679	20040614	17.65 ± 0.05	17.08 ± 0.04	16.50 ± 0.03	SpeX	20050811
J173101.41+531047.9	21.55 ± 0.14	19.34 ± 0.07	1336	20000404	16.32 ± 0.03	15.50 ± 0.03	14.78 ± 0.03	UFTI	20050307
J204317.69-155103.4	[23.74 ± 0.71]	19.72 ± 0.10	5415	20050611	16.87 ± 0.03	16.02 ± 0.03	15.41 ± 0.03	UFTI	20050801
J205235.31-160929.8	[22.72 ± 0.23]	19.06 ± 0.05	5421	20050622	16.04 ± 0.04	15.45 ± 0.03	15.00 ± 0.03	SpeX	20050811
J213154.43-011939.3	[22.68 ± 0.31]	20.01 ± 0.10	4822	20040912	17.29 ± 0.03	16.45 ± 0.03	15.75 ± 0.03	UFTI	20050801
J213240.36+102949.4	21.49 ± 0.10	19.25 ± 0.05	2566	20010918	16.38 ± 0.03	15.52 ± 0.03	14.76 ± 0.03	SpeX	20050813
J213352.72+101841.0	21.96 ± 0.16	19.76 ± 0.10	1739	20000927	16.92 ± 0.03	16.19 ± 0.03	15.61 ± 0.03	SpeX	20050813
J232804.58-103845.7	21.44 ± 0.15	19.76 ± 0.12	1891	20001127	16.77 ± 0.03	15.99 ± 0.03	15.20 ± 0.03	SpeX	20050814

^a Bracketed values denote asinh magnitudes of dwarfs not detected in SDSS *i*.^b Photometrically identified M dwarf; no spectrum obtained.^c Photometrically identified mid-L dwarf; no spectrum obtained.^d Photometrically identified early-L dwarf; no spectrum obtained.

TABLE 2
 ADDITIONAL $ZJHK$ PHOTOMETRY

Name	UFTI Z	MKO J	MKO H	MKO K	Instrument	UT Date
2MASS J00345157+0523050	...	15.11 ± 0.03	15.55 ± 0.03	15.96 ± 0.03	UFTI	20040830
SDSS J075840.33+324723.4	16.47 ± 0.05	UFTI	20040329
SDSS J080531.80+481233.0	16.42 ± 0.05	UFTI	20040329
SDSS J093109.56+032732.5	18.40 ± 0.05	UFTI	20040329
SDSS J111010.01+011613.1	18.00 ± 0.05	UFTI	20040222
SDSS J115700.50+061105.2	18.82 ± 0.05	UFTI	20040222
2MASS J12095613-1004008	17.52 ± 0.05	15.55 ± 0.03	15.24 ± 0.03	15.17 ± 0.03	UFTI	20040329
SDSS J133148.90-011651.4	17.04 ± 0.05	UFTI	20040222
SDSS J152103.24+013142.7	17.99 ± 0.05	UFTI	20040222
2MASS J21011544+1756586	...	16.81 ± 0.03	15.89 ± 0.03	15.00 ± 0.03	SpeX	20050814

TABLE 3
SPECTRAL INDICES OF L-T1 DWARFS (GEBALLE ET AL. 2002 SCHEME)

Name	H ₂ O- <i>J</i>		H ₂ O- <i>H</i>		CH ₄ - <i>H</i>		CH ₄ - <i>K</i>		Mean Type ^a	Instrument and UT Date (yyymmdd)
	Index	Type	Index	Type	Index	Type	Index	Type		
SDSS J000250.98+245413.8	1.57	L5	0.97	<T0	L5 ± 1	CGS4 <i>H</i> 050802
SDSS J000250.98+245413.8	1.39	<T0	[2.17]	[T0]	0.91	<T0	1.06	L6	L6 ± 1	SpeX 050813
SDSS J003609.26+241343.3	1.37	<T0	1.59	L5	0.97	<T0	1.06	L6	L5.5	SpeX 050811
SDSS J020608.97+223559.2	1.40	<T0	1.56	L5	0.92	<T0	1.04	L6	L5.5	SpeX 050123
SDSS J024256.98+212319.6	1.31	<T0	1.53	<T0	1.02	L4	0.92	L3.5	L4	SpeX 051105
SDSS J035104.37+481046.8	2.14	T2.5	2.81	T2	1.18	T1.5	1.11	L7.5	T1 ± 2	SpeX 050121
SDSS J065405.63+652805.4	1.29	<T0	[1.28]	[L0.5]	0.97	...	1.04	L6	L6	SpeX 050123
SDSS J074007.30+200921.9	1.56	L5	0.99	<T0	1.13	L7.5	L6 ± 1.5	CGS4 <i>H</i> 040920, <i>K</i> 040916
SDSS J075656.54+231458.5	1.44	L2.5	0.94	<T0	0.98	L4.5	L3.5 ± 1	CGS4 <i>H,K</i> 040916
SDSS J080531.80+481233.0	1.49	<T0	1.12	T1	1.14	L8	L9.5 ± 1.5	SpeX 050122
SDSS J080959.01+443422.2	1.45	<T0	1.63	L6	0.96	<T0	1.02	L5.5	L6	CGS4 <i>J</i> 040119, UIST <i>HK</i> 040422
SDSS J082030.12+103737.0	1.46	<T0	2.59	T1.5	0.99	<T0	1.12	L7.5	L9.5 ± 2	SpeX 050407
SDSS J083506.16+195304.4	1.38	<T0	1.54	L4.5	0.97	<T0	0.99	L5	L4.5	SpeX 050123
SDSS J085116.20+181730.0	1.48	<T0	1.63	L6	0.97	<T0	0.91	<L3	L4.5 ± 1.5	SpeX 050406
SDSS J085834.42+325627.7	2.06	T0	1.06	T0.5	1.08	L6.5	L9 ± 1.5	UIST <i>HK</i> 040409
SDSS J085834.42+325627.7	1.84	T1	2.03	T0	1.05	T0	1.07	L6.5	L9 ± 1.5	SpeX 050123
SDSS J100711.74+193056.2	1.59	T0	1.74	L8	1.01	<T0	1.07	L6.5	L8 ± 1.5	SpeX 050406
SDSS J102552.43+321234.0	1.57	L5	1.05	T0	L7.5 ± 2.5	CGS4 <i>H</i> 041229
SDSS J102552.43+321234.0	1.64	T0	1.55	L4.5	0.99	<T0	1.04	L5.5	L6.5 ± 2.5	SpeX 050123
SDSS J103321.92+400549.5	1.41	<T0	1.63	L6	0.89	<T0	1.02	L5.5	L6	SpeX 050408
SDSS J103931.35+325625.5	2.15	T0.5	1.17	T1.5	T1	CGS4 <i>H</i> 041229
SDSS J103931.35+325625.5	1.92	T1.5	2.76	T2	1.07	T0.5	1.44	T1	T1	SpeX 050122
SDSS J104335.08+121314.1	1.63	L6	0.97	<T0	1.17	L8.5	L7 ± 1	UIST <i>HK</i> 040406
SDSS J105213.51+442255.7	1.86	T1.5	1.87	L9	1.09	T0.5	1.26	L9.5	T0 ± 1	CGS4 <i>J</i> 040430, UIST <i>HK</i> 040405
SDSS J111320.16+343057.9	1.33	<T0	1.47	L3	0.85	<T0	0.86	<L3	L3	SpeX 050408
SDSS J112118.57+433246.5	1.42	<T0	1.68	L7	0.96	<T0	1.14	L8	L7.5	SpeX 050406
SDSS J121659.17+300306.3	1.34	<T0	1.42	L2.5	0.98	<T0	0.99	L4.5	L3.5 ± 1	SpeX 050408
SDSS J121951.45+312849.4	1.79	L8.5	0.96	<T0	1.15	L8	L8	UIST <i>HK</i> 040703
SDSS J134203.11+134022.2	1.21	<T0	1.57	L5	0.97	<T0	1.05	L6	L5.5	SpeX 050406
SDSS J134525.57+521634.0	1.37	<T0	1.47	L3	0.94	<T0	0.94	L3.5	L3.5	SpeX 050408
SDSS J140023.12+433822.3	1.65	L6.5	[1.04]	[T0]	1.13	L7.5	L7 ± 1	UIST <i>HK</i> 040409
SDSS J140255.66+080055.2	2.06	T0	1.25	T2	1.40	T0.5	T1+/-1	UIST <i>HK</i> 040429
SDSS J140255.87+080055.6	2.27	T0.5	1.19	T1.5	1.43	T0.5	T1	UIST <i>HK</i> 040511
SDSS J141659.78+500626.4	1.40	<T0	1.73	L8	1.01	<T0	0.99	L5	L6.5 ± 1.5	SpeX 050408
SDSS J141659.78+500626.4	1.50	L3.5	1.01	<T0	1.01	L5	L4.5 ± 1	UIST <i>HK</i> 040604
SDSS J142227.25+221557.1	1.17	<T0	1.55	L4.5	1.01	<T0	1.17	L8.5	L6.5 ± 2	SpeX 050406
SDSS J144128.52+504600.4	1.46	L3	0.97	<T0	0.95	L3.5	L3	UIST <i>HK</i> 040426
SDSS J151114.66+060742.9	1.92	T1.5	1.82	L8.5	1.21	T2	1.11	L7	T0 ± 2	SpeX 050406
SDSS J151506.11+443648.3	1.90	L9	1.01	<T0	1.05	L6	L7.5 ± 1.5	UIST <i>HK</i> 040428
SDSS J151643.01+305344.4	2.94	T2.5	0.97	<T0	1.28	L9.5	T1 ± 1.5	UIST <i>HK</i> 040605
SDSS J152039.82+354619.8	1.38	<T0	1.84	L9	1.02	L9.5	1.25	L9.5	L9.5	CGS4 <i>J</i> 040622, UIST <i>HK</i> 040405
SDSS J153453.33+121949.2	1.38	<T0	1.44	L2.5	1.00	<T0	1.02	L5.5	L4 ± 1.5	SpeX 050812
SDSS J154009.36+374230.3	1.40	<T0	2.48	T1.5	0.88	<T0	1.09	L7	L9 ± 1.5	SpeX 050813
SDSS J154508.93+355527.3	1.70	L7.5	[1.03]	[T0]	1.14	L8	L7.5	UIST <i>HK</i> 040617
SDSS J154849.02+172235.4	1.27	<T0	1.60	L5.5	0.94	<T0	0.99	L5	L5	SpeX 050406

TABLE 3 — *Continued*

Name	H ₂ O- <i>J</i>		H ₂ O- <i>H</i>		CH ₄ - <i>H</i>		CH ₄ - <i>K</i>		Mean Type ^a	Instrument and UT Date (yyymmdd)
	Index	Type	Index	Type	Index	Type	Index	Type		
SDSS J161731.65+401859.7	[1.52]	[L9.5]	1.55	L4.5	0.98	<T0	0.94	L3.5	L4	SpeX 050407
SDSS J162051.17+323732.1	1.06	L6	L6	CGS4 <i>K</i> 040916
SDSS J162255.27+115924.1	1.41	<T0	1.69	L7.5	0.90	<T0	0.99	L5	L6 ± 1.5	SpeX 050408
SDSS J163359.23-064056.5	1.40	<T0	[2.03]	[T0]	0.88	L6	1.04	L6	L6	SpeX 050812
SDSS J164916.89+464340.0	1.44	<T0	1.55	L4.5	0.99	<T0	1.04	L6	L5	SpeX 050813
SDSS J171147.17+233130.5	1.06	<T0	1.39	L2	[1.04]	[T0]	1.02	L5.5	L3.5 ± 1.5	SpeX 050814
SDSS J173101.41+531047.9	1.50	<T0	1.70	L7.5	0.98	<T0	0.98	L4.5	L6 ± 1.5	SpeX 050407
SDSS J204317.69-155103.4	1.82	L8.5	1.01	<T0	L8.5 ± 1	CGS4 <i>H</i> 050802
SDSS J204317.69-155103.4	1.53	L9.5	1.74	L8	1.06	T0	1.29	T0	L9.5 ± 1	SpeX 050812
SDSS J205235.31-160929.8	1.58	T0	1.84	L9	1.07	T0.5	1.28	L9.5	L9.5	SpeX 050812
2MASS J21011544+1756586	1.30	<T0	[2.10]	[T0]	0.92	<T0	1.06	L6.5	L6.5 ± 1	SpeX 050814
SDSS J213154.43-011939.3	1.95	L9.5	0.88	<T0	L9.5 ± 1	CGS4 <i>H</i> 050801
SDSS J213154.43-011939.3	1.50	<T0	1.88	L9	0.94	<T0	1.14	L8	L8.5	SpeX 050811
SDSS J213240.36+102949.4	1.46	<T0	1.61	L5.5	0.91	<T0	0.95	L3.5	L4.5 ± 1	SpeX 050813
SDSS J213352.72+101841.0	1.30	<T0	1.52	L4	0.97	<T0	1.04	L6	L5 ± 1	SpeX 050813
SDSS J232804.58-103845.7	1.33	<T0	1.50	L3.5	0.97	<T0	0.93	L3.5	L3.5	SpeX 050814

^a Uncertainties in mean types are ±0.5 subtype, unless otherwise noted.

TABLE 4
SPECTRAL INDICES OF L8–T DWARFS (BURGASSER ET AL. 2005 SCHEME)

Name	H ₂ O- <i>J</i>		CH ₄ - <i>J</i>		H ₂ O- <i>H</i>		CH ₄ - <i>H</i>		CH ₄ - <i>K</i>		Mean Type ^a	Instrument and UT Date (yyymmdd)
	Index	Type										
SDSS J011912.22+240331.6	0.42	T3	0.59	T2.5	0.47	T2.5	0.93	T1.5	0.63	T1.5	T2	SpeX 050812
SDSS J024749.90–163112.6	0.41	T3	0.44	T4.5	0.63	T0	0.85	T2	0.72	T1	T2 ± 1.5	SpeX 050814
SDSS J032553.17+042540.1	0.20	T5.5	0.39	T5	0.28	T6	0.35	T5.5	0.20	T5	T5.5	SpeX 050813
SDSS J035104.37+481046.8	0.48	T2	0.64	T2	0.56	T1	0.85	T2	0.90	<T0	T1 ± 1	SpeX 050121
SDSS J073922.26+661503.5	0.61	<T2	0.75	T0	0.46	T2.5	0.85	T2	0.59	T2	T1.5 ± 1	SpeX 050406
SDSS J080531.80+481233.0	0.70	<T2	0.78	≤T0	0.61	T0.5	0.90	T1.5	0.88	<T0	T0.5 ± 1	SpeX 050122
SDSS J082030.12+103737.0	0.61	<T2	0.70	T1	0.63	T0	1.01	<T0	0.89	<T0	<T0	SpeX 050407
SDSS J085834.42+325627.7	0.60	T0.5	0.94	T1	0.93	<T0	T0.5	UIST HK 040409
SDSS J085834.42+325627.7	0.55	T1.5	0.69	T1	0.55	T1	0.95	T1	0.94	<T0	T1	SpeX 050123
SDSS J090900.73+652527.2	0.54	T1.5	0.71	T1	0.48	T2	0.84	T2	0.59	T2	T1.5	SpeX 050123
SDSS J100711.74+193056.2	0.65	<T2	0.80	<T0	0.60	L9.5	0.99	T0	0.94	<T0	<T0	SpeX 050406
SDSS J103931.35+325625.5	0.61	T0.5	0.85	T2	T1	CGS4 H 041229
SDSS J103931.35+325625.5	0.54	T1.5	0.66	T1.5	0.59	T0.5	0.94	T1	0.69	T1	T1	SpeX 050122
SDSS J104829.21+091937.8	0.47	T2.5	0.48	T4	0.51	T2	0.83	T2.5	0.55	T2.5	T2.5 ± 1	CGS4 J 040514, U
SDSS J105213.51+442255.7	0.57	<T2	0.60	T2	0.68	<T0	0.92	T1.5	0.80	T0	T0.5 ± 1	CGS4 J 040430, U
SDSS J120602.51+281328.7	0.51	T2	0.61	T3.5	T3	CGS4 H 050306
SDSS J120602.51+281328.7	0.45	T2.5	0.55	T3	0.46	T2.5	0.71	T3	0.47	T3	T2.5	SpeX 050408
2MASS J12095613–1004008	0.44	T2.5	0.47	T4	0.46	T2.5	0.67	T3	0.49	T3	T3	CGS4 Z 040627, J
SDSS J121440.95+631643.4	0.34	T4	0.63	T2	0.35	T5	0.71	T3	0.38	T3	T3.5 ± 1	SpeX 050123
SDSS J121951.45+312849.4	0.61	T0.5	1.04	<T0	0.87	<T0	<T0	UIST HK 040703
SDSS J125011.65+392553.9	0.36	T4	0.47	T4	0.39	T4	0.53	T4	0.23	T4.5	T4	CGS4 J 040513, U
SDSS J135852.68+374711.9	0.30	T4.5	0.43	T4.5	T4.5	CGS4 J 040531
SDSS J135852.68+374711.9	0.31	T4.5	0.63	T2	0.36	T4.5	0.36	T5.5	0.29	T4	T4 ± 1	SpeX 050408
SDSS J140255.66+080055.2	0.54	T1.5	0.80	T2.5	0.72	T1	T1.5	UIST HK 040429
SDSS J140255.66+080055.2	0.57	T1	0.84	T2	0.70	T1	T1.5	UIST HK 040511
SDSS J141530.05+572428.7	0.37	T3.5	0.48	T4	0.48	T2	0.63	T3.5	0.66	T1.5	T3 ± 1	CGS4 J 040609, U
SDSS J143553.25+112948.6	0.55	T1	0.88	T2	T1.5	CGS4 H 041229
SDSS J143553.25+112948.6	0.41	T3	0.56	T3	0.49	T2	0.75	T3	0.70	T1	T2.5 ± 1	SpeX 050407
SDSS J143945.86+304220.6	0.57	T1	0.70	T3	T2 ± 1	CGS4 H 041229
SDSS J143945.86+304220.6	0.45	T2.5	0.59	T2.5	0.49	T2	0.72	T3	0.53	T2.5	T2.5	SpeX 050123
SDSS J150411.63+102718.4	0.08	T7.5	0.26	T7	0.24	T7	0.19	T7	0.13	T6.5	T7	CGS4 J 040613, U
SDSS J151114.66+060742.9	0.67	<T2	0.84	<T0	0.67	<T0	0.83	T2	0.90	<T0	T0?	SpeX 050406
SDSS J151643.01+305344.4	0.49	T2	1.03	<T0	0.78	T0	T0.5 ± 1	UIST HK 040605
SDSS J152039.82+354619.8	0.76	<T2	0.68	T1.5	0.69	<T0	0.98	T0.5	0.80	T0	T0 ± 1	CGS4 J 040622, U
SDSS J153417.05+161546.1AB	0.34	T4	0.52	T3.5	0.39	T4	0.72	T3	0.56	T2.5	T3.5	SpeX 050406
SDSS J154009.36+374230.3	0.61	<T2	0.59	T2.5	0.76	<T0	1.14	<T0	0.92	<T0	...	SpeX 050813
SDSS J162838.77+230821.1	0.07	T7.5	0.22	T7.5	0.28	T6	0.19	T7	T7	CGS4 J 040729, H
SDSS J163022.92+081822.0	0.29	T4.5	0.35	T5.5	0.32	T5.5	0.37	T5.5	0.17	T5.5	T5.5	CGS4 J 040502, U
SDSS J204317.69–155103.4	0.69	<T2	0.66	T1.5	0.66	<T0	0.95	T1	0.77	T0	T0.5 ± 1	SpeX 050812
SDSS J205235.31–160929.8	0.67	<T2	0.56	T3	0.67	<T0	0.93	T1.5	0.78	T0	T1 ± 1	SpeX 050812
SDSS J212413.89+010000.3	0.25	T5	0.33	T6	0.42	T3.5	0.43	T5	0.20	T5	T5 ± 1	SpeX 050811
SDSS J213154.43–011939.3	0.67	<T0	1.13	<T0	CGS4 H 050801
SDSS J213154.43–011939.3	0.68	<T2	0.71	T1	0.58	T1	1.07	<T0	0.88	<T0	T0?	SpeX 050811

^a Uncertainties in mean types are ±0.5 subtype, unless otherwise noted.

TABLE 5
 L AND T DWARF COLORS VERSUS SPECTRAL TYPE

Name	Type ^a	<i>i</i> – <i>z</i> ^b	<i>z</i> – <i>J</i>	<i>J</i> – <i>H</i>	<i>H</i> – <i>K</i>	<i>J</i> – <i>K</i>	<i>J</i> ^c
SDSS J111320.16+343057.9	L3.0	2.23 ± 0.16	2.84 ± 0.08	0.92 ± 0.04	0.74 ± 0.04	1.66 ± 0.04	16.92
SDSS J144128.52+504600.4	L3.0	1.96 ± 0.17	3.01 ± 0.09	0.88 ± 0.04	0.80 ± 0.04	1.68 ± 0.04	16.86
SDSS J075656.54+231458.5	L3.5 ± 1.0	> 2.68	3.02 ± 0.07	0.98 ± 0.04	0.82 ± 0.04	1.80 ± 0.04	16.80
SDSS J121659.17+300306.3	L3.5 ± 1.0	2.70 ± 0.26	2.82 ± 0.11	0.70 ± 0.06	0.63 ± 0.04	1.33 ± 0.06	16.89
SDSS J134525.57+521634.0	L3.5	2.18 ± 0.20	2.79 ± 0.10	0.75 ± 0.04	0.76 ± 0.04	1.51 ± 0.04	17.05
SDSS J171147.17+233130.5	L3.5 ± 1.5	1.95 ± 0.27	3.11 ± 0.13	0.84 ± 0.04	0.75 ± 0.04	1.59 ± 0.04	16.84
SDSS J232804.58–103845.7	L3.5	1.68 ± 0.19	2.99 ± 0.12	0.78 ± 0.04	0.79 ± 0.04	1.57 ± 0.04	16.77
SDSS J153453.33+121949.2	L4.0 ± 1.5	2.30 ± 0.06	2.91 ± 0.04	0.85 ± 0.04	0.73 ± 0.04	1.58 ± 0.04	15.27
SDSS J161731.65+401859.7	L4.0	2.28 ± 0.19	2.98 ± 0.10	1.14 ± 0.04	0.85 ± 0.04	1.99 ± 0.04	16.83
SDSS J024256.98+212319.6	L4.0	2.22 ± 0.20	2.97 ± 0.09	0.86 ± 0.04	0.76 ± 0.04	1.62 ± 0.04	17.05
SDSS J083506.16+195304.4	L4.5	2.26 ± 0.09	2.90 ± 0.06	0.82 ± 0.04	0.71 ± 0.04	1.53 ± 0.04	15.94
SDSS J085116.20+181730.0	L4.5 ± 1.5	2.24 ± 0.17	3.00 ± 0.09	0.88 ± 0.05	0.83 ± 0.05	1.71 ± 0.04	16.68
SDSS J213240.36+102949.4	L4.5 ± 1.0	2.24 ± 0.11	2.87 ± 0.06	0.86 ± 0.04	0.76 ± 0.04	1.62 ± 0.04	16.38
SDSS J154849.02+172235.4	L5.0	2.50 ± 0.08	2.73 ± 0.05	0.85 ± 0.04	0.75 ± 0.04	1.60 ± 0.04	16.09
SDSS J164916.89+464340.0	L5.0	2.66 ± 0.21	2.64 ± 0.09	0.76 ± 0.04	0.59 ± 0.04	1.35 ± 0.04	17.09
SDSS J213352.72+101841.0	L5.0 ± 1.0	2.20 ± 0.19	2.84 ± 0.10	0.73 ± 0.04	0.58 ± 0.04	1.31 ± 0.04	16.92
SDSS J000250.98+245413.8	L5.5	2.21 ± 0.18	2.97 ± 0.09	0.93 ± 0.04	0.67 ± 0.04	1.60 ± 0.04	17.02
SDSS J003609.26+241343.3	L5.5	> 2.43	2.99 ± 0.12	0.80 ± 0.06	0.80 ± 0.04	1.60 ± 0.06	17.08
SDSS J020608.97+223559.2	L5.5	3.17 ± 0.17	2.91 ± 0.05	0.75 ± 0.05	0.56 ± 0.05	1.30 ± 0.05	16.34
SDSS J134203.11+134022.2	L5.5	2.45 ± 0.22	2.96 ± 0.09	0.95 ± 0.04	0.82 ± 0.04	1.77 ± 0.04	16.90
SDSS J141659.78+500626.4	L5.5 ± 2.0	2.48 ± 0.25	2.91 ± 0.10	0.76 ± 0.05	0.68 ± 0.04	1.44 ± 0.05	16.79
SDSS J173101.41+531047.9	L6.0 ± 1.5	2.21 ± 0.16	3.02 ± 0.08	0.82 ± 0.04	0.72 ± 0.04	1.54 ± 0.04	16.32
SDSS J065405.63+652805.4	L6.0 ± 1.0	2.08 ± 0.06	2.81 ± 0.05	0.73 ± 0.04	0.76 ± 0.04	1.49 ± 0.04	16.08
SDSS J074007.30+200921.9	L6.0 ± 1.5	> 2.72	3.11 ± 0.10	0.85 ± 0.04	0.71 ± 0.04	1.56 ± 0.04	16.67
SDSS J080959.01+443422.2	L6.0	2.54 ± 0.17	2.91 ± 0.07	1.12 ± 0.04	0.94 ± 0.04	2.06 ± 0.04	16.37
SDSS J103321.92+400549.5	L6.0	2.40 ± 0.17	2.80 ± 0.07	0.69 ± 0.05	0.45 ± 0.06	1.14 ± 0.06	16.74
SDSS J162051.17+323732.1	L6.0	> 2.49	2.84 ± 0.12	0.94 ± 0.05	0.83 ± 0.04	1.77 ± 0.05	17.17
SDSS J162255.27+115924.1	L6.0 ± 1.5	2.50 ± 0.18	2.54 ± 0.08	0.74 ± 0.06	0.69 ± 0.04	1.43 ± 0.06	16.89
SDSS J163359.23–064056.5	L6.0	2.55 ± 0.09	2.76 ± 0.05	0.75 ± 0.04	0.71 ± 0.04	1.46 ± 0.04	16.00
SDSS J142227.25+221557.1	L6.5 ± 2.0	2.45 ± 0.17	2.84 ± 0.09	0.75 ± 0.04	0.48 ± 0.04	1.23 ± 0.04	16.87
2MASS J21011544+1756586	L6.5 ± 1.0	2.76 ± 0.28	2.87 ± 0.09	0.92 ± 0.04	0.89 ± 0.04	1.81 ± 0.04	16.81
SDSS J104335.08+121314.1	L7.0 ± 1.0	3.13 ± 0.19	3.04 ± 0.05	0.95 ± 0.04	0.67 ± 0.04	1.62 ± 0.04	15.82
SDSS J140023.12+433822.3	L7.0 ± 1.0	> 3.42	2.92 ± 0.05	0.98 ± 0.04	0.71 ± 0.04	1.69 ± 0.04	16.16
SDSS J102552.43+321234.0	L7.5 ± 2.5	> 2.81	2.80 ± 0.09	0.91 ± 0.06	0.82 ± 0.04	1.73 ± 0.06	16.89
SDSS J112118.57+433246.5	L7.5	2.38 ± 0.21	2.89 ± 0.10	0.48 ± 0.06	0.43 ± 0.06	0.91 ± 0.06	17.04
SDSS J151506.11+443648.3	L7.5 ± 1.5	2.57 ± 0.16	2.96 ± 0.07	0.91 ± 0.04	0.77 ± 0.04	1.68 ± 0.04	16.54
SDSS J154508.93+355527.3	L7.5	2.41 ± 0.20	2.90 ± 0.09	0.93 ± 0.04	0.75 ± 0.04	1.68 ± 0.04	16.97
SDSS J100711.74+193056.2	L8.0 ± 1.5	> 2.74	3.01 ± 0.10	0.90 ± 0.07	0.70 ± 0.06	1.60 ± 0.06	16.75
SDSS J121951.45+312849.4	L8.0	3.12 ± 0.16	3.00 ± 0.05	0.87 ± 0.04	0.68 ± 0.04	1.55 ± 0.04	15.85
SDSS J154009.36+374230.3	L9.0 ± 1.5	> 3.47	2.70 ± 0.07	0.91 ± 0.04	0.77 ± 0.04	1.68 ± 0.04	16.33
SDSS J204317.69–155103.4	L9.0	> 2.78	2.85 ± 0.10	0.85 ± 0.04	0.61 ± 0.04	1.46 ± 0.04	16.87
SDSS J213154.43–011939.3	L9.0	> 2.49	2.72 ± 0.10	0.84 ± 0.04	0.70 ± 0.04	1.54 ± 0.04	17.29
SDSS J080531.80+481233.0	L9.5 ± 1.5	2.20 ± 0.05	3.01 ± 0.04	0.60 ± 0.04	0.50 ± 0.04	1.10 ± 0.04	14.61
SDSS J082030.12+103737.0	L9.5 ± 2.0	> 2.47	3.00 ± 0.09	0.94 ± 0.06	0.51 ± 0.06	1.45 ± 0.04	17.03
SDSS J151114.66+060742.9	T0.0 ± 2.0	2.79 ± 0.20	3.26 ± 0.07	0.67 ± 0.04	0.64 ± 0.04	1.31 ± 0.04	15.83
SDSS J152039.82+354619.8	T0.0 ± 1.0	3.55 ± 0.12	2.84 ± 0.04	0.91 ± 0.04	0.54 ± 0.04	1.45 ± 0.04	15.47
SDSS J105213.51+442255.7	T0.5 ± 1.0	> 3.39	3.22 ± 0.07	0.80 ± 0.04	0.63 ± 0.04	1.43 ± 0.04	15.89
SDSS J151643.01+305344.4	T0.5 ± 1.0	> 2.51	3.20 ± 0.11	0.93 ± 0.04	0.74 ± 0.04	1.67 ± 0.04	16.79
SDSS J035104.37+481046.8	T1.0 ± 1.5	> 2.93	3.28 ± 0.07	0.48 ± 0.05	0.63 ± 0.05	1.11 ± 0.05	16.29
SDSS J085834.42+325627.7	T1.0	3.02 ± 0.16	2.74 ± 0.06	0.88 ± 0.04	0.73 ± 0.04	1.61 ± 0.04	16.33
SDSS J103931.35+325625.5	T1.0	> 3.09	3.25 ± 0.07	0.69 ± 0.04	0.46 ± 0.04	1.15 ± 0.04	16.16
SDSS J205235.31–160929.8	T1.0 ± 1.0	> 3.44	3.02 ± 0.06	0.59 ± 0.05	0.45 ± 0.04	1.04 ± 0.05	16.04
SDSS J073922.26+661503.5	T1.5 ± 1.0	> 2.64	3.11 ± 0.09	0.44 ± 0.04	0.26 ± 0.04	0.70 ± 0.04	16.75
SDSS J090900.73+652527.2	T1.5	> 3.75	2.94 ± 0.06	0.49 ± 0.04	0.13 ± 0.04	0.62 ± 0.04	15.81
SDSS J140255.66+080055.2	T1.5	> 2.57	3.08 ± 0.09	0.60 ± 0.04	0.52 ± 0.04	1.12 ± 0.04	16.85
SDSS J011912.22+240331.6	T2.0	> 2.04	3.60 ± 0.11	0.40 ± 0.04	0.20 ± 0.04	0.60 ± 0.04	16.86
SDSS J024749.90–163112.6	T2.0 ± 1.5	> 2.67	3.10 ± 0.11	0.42 ± 0.04	0.50 ± 0.04	0.92 ± 0.04	16.73
SDSS J143553.25+112948.6	T2.0 ± 1.0	> 2.37	3.09 ± 0.10	0.52 ± 0.05	0.37 ± 0.07	0.89 ± 0.07	17.04
SDSS J104829.21+091937.8	T2.5	> 2.81	3.30 ± 0.09	0.44 ± 0.04	0.08 ± 0.04	0.52 ± 0.04	16.39
SDSS J143945.86+304220.6	T2.5	> 2.26	3.27 ± 0.10	0.44 ± 0.04	0.19 ± 0.06	0.63 ± 0.06	16.97
SDSS J120602.51+281328.7	T3.0	> 3.02	3.38 ± 0.08	0.27 ± 0.04	–0.14 ± 0.04	0.13 ± 0.04	16.10
2MASS J12095613–1004008	T3.0	0.31 ± 0.04	0.07 ± 0.04	0.38 ± 0.04	15.55
SDSS J141530.05+572428.7	T3.0 ± 1.0	> 2.63	3.38 ± 0.09	0.40 ± 0.04	0.54 ± 0.04	0.94 ± 0.04	16.49

TABLE 5 — *Continued*

Name	Type ^a	$i-z$ ^b	$z-J$	$J-H$	$H-K$	$J-K$	J^c
SDSS J121440.95+631643.4	$T3.5 \pm 1.0$	> 2.85	3.60 ± 0.10	0.25 ± 0.04	0.07 ± 0.05	0.32 ± 0.05	16.05
SDSS J153417.05+161546.1AB ^d	T3.5	> 2.30	3.58 ± 0.12	0.25 ± 0.04	0.31 ± 0.04	0.56 ± 0.04	16.62
SDSS J125011.65+392553.9	T4.0	> 2.55	3.83 ± 0.09	0.05 ± 0.04	0.00 ± 0.04	0.05 ± 0.04	16.12
SDSS J135852.68+374711.9	$T4.5 \pm 1.0$	> 2.61	3.72 ± 0.09	-0.24 ± 0.04	-0.25 ± 0.06	-0.49 ± 0.06	16.17
SDSS J212413.89+010000.3	T5.0	> 2.79	3.83 ± 0.12	-0.24 ± 0.04	0.05 ± 0.04	-0.19 ± 0.04	15.88
SDSS J032553.17+042540.1	T5.5	> 2.75	3.85 ± 0.09	-0.35 ± 0.04	-0.22 ± 0.05	-0.57 ± 0.05	15.88
SDSS J163022.92+081822.0	T5.5	> 2.37	3.95 ± 0.10	-0.17 ± 0.04	-0.06 ± 0.04	-0.23 ± 0.04	16.18
2MASS J00345157+0523050 ^e	T6.5	-0.44 ± 0.04	-0.41 ± 0.04	-0.85 ± 0.04	15.11
SDSS J150411.63+102718.4	T7.0	> 2.16	3.85 ± 0.14	-0.43 ± 0.04	-0.10 ± 0.04	-0.53 ± 0.04	16.49
SDSS J162838.77+230821.1	T7.0	> 2.27	3.98 ± 0.10	-0.38 ± 0.05	-0.09 ± 0.05	-0.47 ± 0.04	16.25
.							

^a Uncertainties in spectral types are ± 0.5 subtype, unless otherwise noted.

^b $i-z$ colors of dwarfs not detected in i are calculated using 5σ detection limit of $i = 22.5$, and indicated with “ $>$ ” as lower limits.

^c J photometry errors are typically 0.03 mag, also refer to Table 1.

^d Identified by Liu et al. 2006 as a close binary with T1-T2 and T5-T6 components

^e Spectral type from Burgasser et al. (2005)